Tailoring Size Effects on the Exchange Bias in Ferromagnetic-Antiferromagnetic < 100 nm Nanostructures

Vincent Baltz, J. Sort, S. Landis, B. Rodmacq, B. Dieny

Tailoring Size Effects on the Exchange Bias in Ferromagnetic-Antiferromagnetic <100 nm Nanostructures

V. Baltz,[1,*] J. Sort,[1] S. Landis,[2] B. Rodmacq,[1] and B. Dieny[1]
[1]SPINTEC (URA 2512), CEA/CNRS, 17 Av. Martyrs, 38054 Grenoble Cedex 9, France
[2]LETI/D2NT, CEA, 17 Av. Martyrs, 38054 Grenoble Cedex 9, France
(Received 16 July 2004; published 22 March 2005)

The hysteresis loop shift in sub-100 nm ferromagnetic- (FM-)antiferromagnetic (AFM) nanostructures can be either *enhanced* or *reduced* with respect to continuous films with the same composition, with varying the AFM layer thickness. An enhancement of the coercivity and a reduction of the blocking temperature are also observed. These effects are mainly ascribed to the physical limitations that the dot sizes impose on the AFM domain size and the concomitant weakening of the pinning strength exerted by the AFM during magnetization reversal of the FM.

DOI: 10.1103/PhysRevLett.94.117201 PACS numbers: 75.75.+a, 75.60.–d, 75.70.Cn

Exchange bias (EB) refers to the shift of the hysteresis loop along the magnetic field axis observed in exchange interacting ferromagnetic- (FM-)antiferromagnetic (AFM) materials. The loop shift is usually accompanied with an enhancement of coercivity [1]. The majority of theoretical models dealing with EB attribute such effects to the formation of domains and pinning of domain walls (DWs) either in the FM [2,3] or in the AFM layer [4,5].

During recent decades, EB properties have been extensively investigated, mainly in thin films, due to their technological applications in magnetic random access memories and magnetoresistive read heads based on spin valves or tunnel junctions [6]. Recently, the drastic increase in the areal density of magnetic recording media has motivated the study of EB properties in systems of reduced lateral dimensions [7–19]. The reduction of the lateral dimensions of an EB system down to length scales comparable to FM or AFM magnetic domain sizes (typically hundreds of nanometers) is also interesting from a fundamental point of view since this results in a confinement and subsequent alteration of the FM and AFM domain structures [10–13], hence allowing us to probe the role of domains on EB.

Although a considerable number of studies have been reported in the literature on micron or submicron spin valve systems [20], the effects of reduced lateral dimensions on EB have been far less investigated. Yet when the dimensions of the FM-AFM nanostructures are reduced down to the magnetic domain sizes, an enhancement of the coercive field, H_C [8,9,11–14], or changes in the asymmetry of the hysteresis loops have been observed [9,17]. More controversial is the effect of reduced lateral dimensions on the magnitude of the EB field, H_E. Indeed, some authors reported that H_E is enhanced in nanostructures [7–10], whereas others observed the opposite trend [11–18]. Up to now, this discrepancy has been attributed to the different materials or the nanostructuring techniques employed.

In this Letter, we report on the dependence of EB on the AFM and FM layers thicknesses in sub-100 nm FM-AFM bilayers sputtered on prepatterned Si square dots. We demonstrate that, at room temperature, although all samples were fabricated using the same lithography technique and all of them consist of the same FM and AFM materials, it is possible to either *enhance* or *reduce* the magnitude of H_E in the nanostructures, with respect to continuous films with the same composition, by varying the thickness of the AFM layer, while keeping the dot size constant. Such a behavior is not observed when varying the FM thickness.

To fabricate the nanostructures, Si wafers were first patterned by electron beam lithography and reactive ion etching to form arrays of Si square dots with lateral sizes of 90 nm, height of 300 nm, and periodicity of 200 nm [see inset of Fig. 1(a)]. Two series of multilayers with compositions Ta (5 nm)/Py (12 nm)/IrMn (t_{IrMn})/Pt (2 nm) and Ta (5 nm)/Py (t_{Py})/IrMn (5 nm)/Pt (2 nm) (where Py is permalloy: $Ni_{81}Fe_{19}$ and IrMn stands for $Ir_{20}Mn_{80}$) were

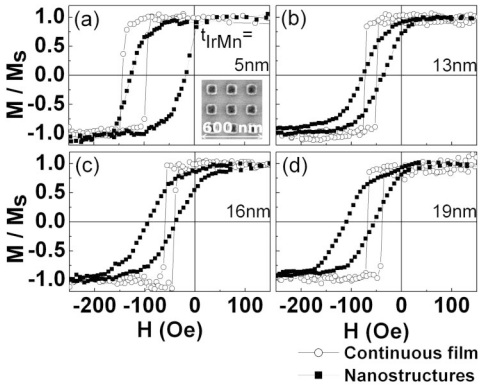

FIG. 1. Hysteresis loops of the continuous films (- ○ -) and the nanostructures (-■-), with compositions Ta (5 nm)/Py (12 nm)/IrMn (t_{IrMn})/Pt (2 nm) (for t_{IrMn} = 5, 13, 16, and 19 nm), measured at room temperature by longitudinal Kerr effect along the field cooling direction, after cooling from $T = 550$ K in the presence of a 2.4 kOe field. The inset is a scanning electron microscopy (SEM) image of the nanostructures. 1

deposited, simultaneously, on unpatterned and patterned Si wafers by dc magnetron sputtering. All the samples were grown at room temperature under a 0.25 Pa Ar pressure with deposition rates of about 0.08 nm s^{-1} [21]. The IrMn and Py thicknesses, t_{IrMn} and t_{Py}, were varied from 5 nm to 19 nm and 6 nm to 20 nm, respectively. This nanostructuring technique allows the direct deposition of the magnetic material on the prepatterned substrates, hence avoiding possible degradation effects due to post-deposition etching, such as partial structural deterioration of the layers [21,22]. To set EB, the samples were post-annealed and field cooled from $T = 550$ K (from above the blocking temperature of all systems) under a 2.4 kOe in plane magnetic field, applied parallel to one of the sides of the square dots. Hysteresis loops of both the continuous films and the nanostructures were measured at room temperature along the field cooling direction using a longitudinal Kerr effect setup. The geometry was selected to avoid the magnetic signal from the trenches when measured by Kerr effect. The blocking temperatures in both the dots and the continuous film were evaluated by field cooling the samples under a negative field from temperatures ranging from 300 to 550 K, after the standard cooling procedure.

The hysteresis loops of both the continuous films and the arrays of dots for various t_{IrMn} are plotted in Fig. 1. All the loops display a significant shift along the magnetic field axis. Moreover, the loops of the continuous films remain square with a 100% remanence to saturation ratio. In contrast, the loops corresponding to the nanostructures are somewhat slanted (i.e., they tend to lose their square appearance). Compared to other studies of EB in patterned elements [9,17], no pronounced asymmetries are observed. The loop shearing is ascribed to the switching field distribution for the different dots [22].

Figure 2 shows the dependences of H_E on t_{IrMn} for the continuous films and the nanostructures with compositions Ta (5 nm)/Py (12 nm)/IrMn (t_{IrMn})/Pt (2 nm). The H_E evolutions follow totally different trends in the dots and in the continuous bilayers. Namely, H_E in the continuous films decreases as t_{IrMn} increases whereas H_E in the nanostructures seems to be rather insensitive to t_{IrMn}. As a result, although H_E in the nanostructures is smaller than for the continuous films for thin AFM layers, larger H_E for the dots is observed for large t_{IrMn} values. The decrease of H_E with increasing the AFM layer thickness (t_{AFM}) in the continuous films has already been observed and tentatively explained [5,23–29]. Following the arguments initially proposed by Imry and Ma [24], and using the random field model for FM-AFM exchange biased systems, Malozemoff predicted an inversely proportional relationship between H_E and the AFM layer thickness [5]. His argument is based on the assumption that due to the random coupling through the FM-AFM interface, the AFM spin lattice breaks up into domains, the size of which is determined by a balance between a gain in FM-AFM interfacial energy provided by aligning the local net AFM moment with the FM magnetization and an energy cost due to domain walls (DWs) formation in the AFM. The interfacial coupling energy per unit area is $\sigma_{FM\text{-}AFM} = -J_{FM\text{-}AFM}/(aD_{AFM})$, where $J_{FM\text{-}AFM}$ is the interatomic exchange constant of the FM-AFM coupling, a the distance between AFM spins, and D_{AFM} the AFM domain size. On the other hand, the DW energy per unit area of DW in the AFM can be written as $\sigma_{DW,AFM} = \pi^2 J_{AFM}/(4aD_{AFM})$, where J_{AFM} is the exchange constant of the AFM spins. The equilibrium domain size can be obtained by minimizing the total energy per unit FM-AFM interfacial area $\sigma_{FM\text{-}AFM} + \pi(t_{AFM}/D_{AFM})\sigma_{DW,AFM}$. This yields the following relationship between the AFM domain size and t_{AFM}: $D_{AFM} = \pi^3 J_{AFM} t_{AFM}/(2J_{FM\text{-}AFM})$. Hence, substituting this equation in the above expression of $\sigma_{FM\text{-}AFM}$, the inverse proportionality relation between $\sigma_{FM\text{-}AFM}$ and t_{AFM} is readily obtained, which explains the variation of H_E on t_{IrMn} for continuous FM-AFM bilayers shown in Fig. 2. It is noteworthy that the domain state model for EB can also account for the AFM thickness dependence of H_E [23].

In contrast to continuous films, H_E seems to be roughly independent of t_{AFM} for the nanostructures. This suggests that the mechanism responsible for the H_E reduction in the continuous film is probably not operative in FM-AFM nanostructures. Actually, taking into account reasonable values of $J_{FM\text{-}AFM}$ and J_{AFM} from the literature, i.e., $J_{FM\text{-}AFM} = 7.6 \times 10^{-15}$ erg and $J_{AFM} = 16.1 \times 10^{-15}$ erg [26], one can estimate that D_{AFM} is about 160 nm for $t_{IrMn} = 5$ nm and it increases progressively up to 620 nm for $t_{IrMn} = 19$ nm, which is consistent with direct x-ray photoemission electron microscopy observations [30]. Additionally, taking into account the values of the magnetic stiffness for IrMn ($A_{IrMn} \approx 10^{-6}$ erg cm^{-1})

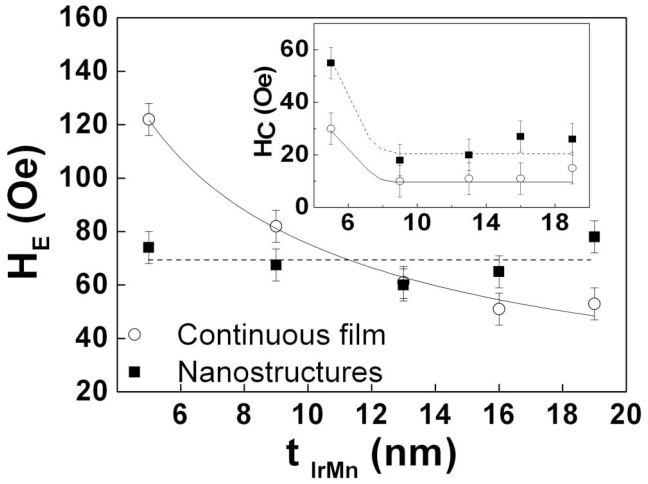

FIG. 2. Dependence of the exchange bias field, H_E, on the IrMn thickness, t_{IrMn}, for both continuous films (-○-) and nanostructures (-■-). The inset shows the dependence of the coercivity, H_C, on t_{IrMn}. The lines are guides to the eye.

and its magnetic anisotropy ($K_{\mathrm{IrMn}} \approx 1.8 \times 10^6$ erg cm^{-3}), the Bloch domain wall width in IrMn, δ_{IrMn}, can be estimated to be $\delta_{\mathrm{IrMn}} \approx \pi(A_{\mathrm{IrMn}}/K_{\mathrm{IrMn}})^{1/2} \approx$ 25 nm [31,32]. Since the dot size is smaller than the AFM domain size, it is likely that only a single AFM domain (with still local variations in the AFM order due to frustrations such as roughness, defects...) can form inside the nanostructures. Hence, for sub-100 nm dots, the lateral dimensions of the dots physically limit the AFM domain size, thus keeping H_E constant for all IrMn thicknesses.

Malozemoff's model provides an estimation of the AFM domain size. However, it is a static model which does not take into account any reorganization of the AFM spin lattice during the magnetization reversal of the FM. The fact that the AFM domain size imposed by the lateral dimensions of the dots is always smaller than D_{AFM} in continuous films but, conversely, that H_E is not always larger in the nanostructures, seems to indicate that the AFM spin structure is less effectively pinned in the nanostructures than in the continuous films. Evidence for this hypothesis is obtained from the behavior of the blocking temperature, T_B, and the coercivity. The dependence of T_B on t_{IrMn} for the continuous bilayers and the arrays of dots is shown in Fig. 3. The figure reveals that, in both systems, T_B increases with t_{IrMn}, as typically observed in EB bilayers [1]. However, T_B remains lower for the nanostructures in the overall range of t_{IrMn}. Hence, thermal activation effects in the AFM are more pronounced in the nanostructures than in the continuous films. Moreover, a H_C enhancement is observed in the nanostructures with respect to the continuous films (see inset of Fig. 2). This can be ascribed to an AFM spin dragging occurring during the magnetization reversal of the FM, which could be more pronounced in the dots than in continuous films. Interestingly, some published temperature-dependent results on EB in nanostructures [13] also show that, at room temperature, the pinning strength exerted by the AFM can be weaker in the nanostructures. Moreover, at low temperatures, where thermal activation effects are minimized, SQUID measurements also indicate that exchange bias in the nanostructures can be larger than for the continuous films, in agreement with Malozemoff's model prediction (since the dot size, i.e., the AFM domain size in the nanostrucutures, is smaller than the estimated AFM domain size for the continuous films).

The weakening of the pinning strength in the nanostructures could stem from the reduced coordination number of AFM spins located at the edges of the dots. These spins can be more easily rotated during magnetization reversal of the FM. In addition, defects located in the bulk of the AFM layer would, in principle, favor the formation of domain walls in the AFM [33]. However, since the formation of domain walls is energetically unfavorable in the nanostructures, these defects are likely to distort the AFM order only locally, causing local twists of the AFM spins, which can easily unwind during the magnetization reversal of the FM.

It is noteworthy that the difference of blocking temperatures, $\Delta T_B = T_{B,\mathrm{continuous}} - T_{B,\mathrm{dots}}$, increases for low t_{IrMn} values (see inset of Fig. 3), where the H_C enhancement is also more pronounced (see inset of Fig. 2). Additionally, although H_E remains constant at room temperature for all AFM thicknesses, H_E for thin AFM layers becomes progressively further reduced than for thicker AFM layers when the samples are heated again to a certain temperature $T < T_B$ and cooled back to room temperature using negative fields, i.e., when trying to reset exchange bias in the

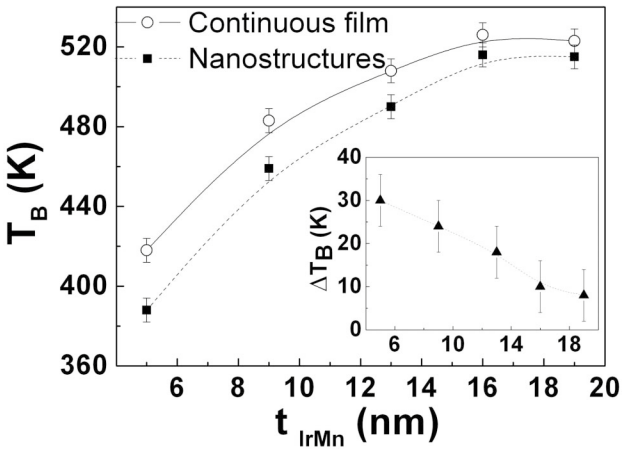

FIG. 3. Dependence of the blocking temperature, T_B, on the IrMn thickness, t_{IrMn}, for the continuous films (-○-) and the nanostructures (-■-). The inset shows the dependence of the relative difference of blocking temperatures between the continuous bilayers and the nanostructures, ΔT_B, on t_{IrMn}. The lines are guides to the eye.

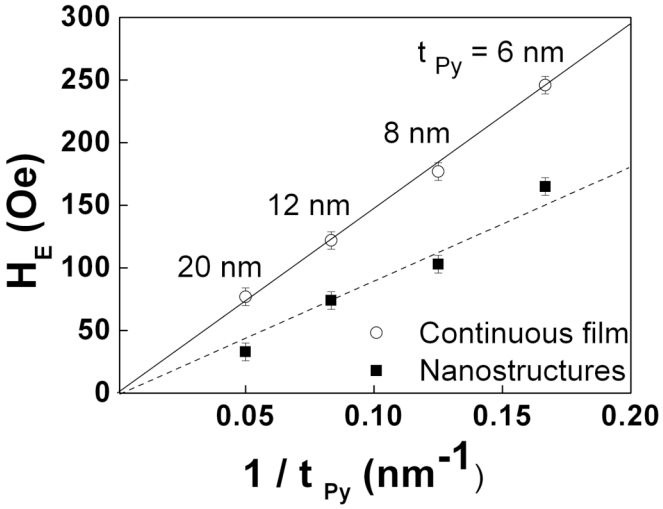

FIG. 4. Dependence of the exchange bias field, H_E, on the Py thickness, t_{Py}, for both the continuous films and the nanostructures with compositions Ta (5 nm)/Py (t_{Py})/IrMn (5 nm)/Pt (2 nm). The full and dashed lines are $1/t_{\mathrm{Py}}$ fits of the H_E evolutions in continuous films and in nanostructures, respectively.

opposite direction. Thus, the relative unpinning of AFM domains in the dots, compared to continuous films, seems slightly more manifest for thin AFM layers. It has to be noted that the technological inconvenience of a T_B reduction in nanostructures can be minimized by using thick AFM layers, where one tends to recover the same T_B as in continuous films.

Figure 4 shows the evolutions of H_E as a function of $1/t_{\mathrm{Py}}$ for continuous films and nanostructures with compositions Ta (5 nm)/Py (t_{Py})/IrMn (5 nm)/Pt (2 nm). In both cases, H_E follows the well known $1/t_{\mathrm{Py}}$ law, as typically observed in EB continuous bilayers [1,28,29,34], but the slopes are different, a consequence of the different FM-AFM coupling strength already discussed for low t_{AFM} values. Up to now, the scaling of this law to small lateral dimensions ended in the micron sized elements range [10,14]. Such $1/t_{\mathrm{FM}}$ evolution of H_E highlights the mainly interfacial character of the FM-AFM coupling in both continuous films and nanostructures.

In conclusion, in sub-100 nm Py/IrMn nanostructures, the hysteresis loop shift can be either *larger* or *smaller* than that of continuous films with the same composition, depending on the AFM layer thickness. An enhancement of the coercivity and a reduction of the blocking temperature were also observed. These effects are ascribed to the three-dimensional confinement of AFM domains in the nanostructures. Our work sheds light towards the understanding of the controversial results published in the literature about the influence of reduced lateral dimensions in FM-AFM systems on EB.

This work was supported by the European Community through the NEXBIAS Grant No. HPRN-CT-2002-00296.

*Electronic address: baltz@drfmc.ceng.cea.fr

[1] For recent reviews on exchange bias, see J. Nogués and I. K. Schuller, J. Magn. Magn. Mater. **192**, 203 (1999); A. E. Berkowitz and K. Takano, *ibid.* **200**, 552 (1999); R. L. Stamps, J. Phys. D: Appl. Phys. **33,** R247 (2000); M. Kiwi, J. Magn. Magn. Mater. **234**, 584 (2001).
[2] M. Kiwi, J. Mejía-López, R. D. Portugal, and R. Ramírez, Europhys. Lett. **48**, 573 (1999).
[3] S. Zhang and Z. Li, Phys. Rev. B **65**, 054406 (2002).
[4] D. Mauri, H. C. Siegmann, P. S. Bagus, and E. Kay, J. Appl. Phys. **62**, 3047 (1987).
[5] A. P. Malozemoff, Phys. Rev. B **35**, 3679 (1987).
[6] B. Dieny, V. S. Speriosu, S. S. P. Parkin, B. A. Gurney, D. R. Wilhoit, and D. Mauri, Phys. Rev. B **43**, 1297 (1991).
[7] A. Nemoto, Y. Otani, S. G. Kim, K. Fukamichi, O. Kitakami, and Y. Shimada, Appl. Phys. Lett. **74**, 4026 (1999).
[8] T. Kimura, G. Mozumi, F. Wakaya, and K. Gamo, Jpn. J. Appl. Phys. **40**, 2241 (2001).
[9] K. Liu, S. M. Baker, M. Tuominen, T. P. Russell, and I. K. Schuller, Phys. Rev. B **63**, 060403 (2001).
[10] J. C. Wu, H. W. Huang, C. H. Lai, and T. H. Wu, J. Appl. Phys. **87**, 4948 (2000).
[11] J. Sort, H. Glaczynska, U. Ebels, B. Dieny, M. Giersig, and J. Rybczynski, J. Appl. Phys. **95**, 7516 (2004).
[12] V. Baltz, J. Sort, B. Rodmacq, B. Dieny, and S. Landis, Appl. Phys. Lett. **84**, 4923 (2004).
[13] M. Fraune, U. Rüdiger, G. Güntherodt, S. Cardoso, and P. Freitas, Appl. Phys. Lett. **77**, 3815 (2000).
[14] J. Yu, A. D. Kent, and S. S. P. Parkin, J. Appl. Phys. **87**, 5049 (2000).
[15] Y. Shen, Y. Wu, H. Xie, K. Li, J. Qiu, and Z. Guo, J. Appl. Phys. **91**, 8001 (2002).
[16] Z. B. Guo, K. B. Li, G. C. Han, Z. Y. Liu, P. Luo, and Y. H. Wu, J. Magn. Magn. Mater. **251**, 323 (2002).
[17] E. Girgis, R. D. Portugal, H. Loosvelt, M. J. Van Bael, I. Gordon, M. Malfait, K. Temst, C. Van Haesendonck, L. H. A. Leunissen, and R. Jonckheere, Phys. Rev. Lett. **91**, 187202 (2003).
[18] A. Hoffmann, M. Grimsditch, J. E. Pearson, J. Nogués, W. A. A. Macedo, and I. K. Schuller, Phys. Rev. B **67**, 220406 (2003).
[19] K. Liu, J. Nogués, C. Leighton, H. Masuda, K. Nishio, I. V. Roshchin, and I. K. Schuller, Appl. Phys. Lett. **81**, 4434 (2002).
[20] S. Tehrani, J. M. Slaughter, M. Deherrera, B. N. Engel, N. D. Rizzo, J. Slater, M. Durlam, R. W. Dave, J. Janesky, B. Butcher, K. Smith, and G. Grynkewich, Proc. IEEE **91**, 703 (2003).
[21] S. Landis, B. Rodmacq, B. Dieny, B. Dal'Zotto, S. Tedesco, and M. Heitzmann, Phys. Rev. B **62**, 12271 (2000).
[22] J. I. Martin, J. Nogués, K. Liu, J. L. Vicent, and I. K. Schuller, J. Magn. Magn. Mater. **256**, 449 (2003).
[23] M. Ali, C. H. Marrows, M. Al-Jawad, B. J. Hickey, A. Mistra, U. Nowak, and K. D. Usabel, Phys. Rev. B **68**, 214420 (2003).
[24] Y. Imry and S.-k. Ma, Phys. Rev. Lett. **35**, 1399 (1975).
[25] T. Ambrose and C. L. Chien, J. Appl. Phys. **83**, 6822 (1998).
[26] H. Xi, J. Rantschler, S. Mao, M. T. Kief, and R. M. White, J. Phys. D: Appl. Phys. **36**, 1464 (2003).
[27] G. Anderson, Y. Huai, and L. Miloslawsky, J. Appl. Phys. **87**, 6989 (2000).
[28] H. Li, P. P. Freitas, Z. Wang, J. B. Sousa, P. Gogol, and J. Chapman, J. Appl. Phys. **89**, 6904 (2001).
[29] T. Lin, C. Tsang, R. E. Fontana, and J. K. Howard, IEEE Trans. Magn. **31**, 2585 (1995).
[30] T. Eimüller, T. Kato, T. Mitzuno, S. Tsunashima, C. Quitmann, T. Ramsvik, S. Iwata, and G. Schütz, Appl. Phys. Lett. **85**, 2310 (2004).
[31] M. J. Carey, N. Smith, B. A. Gurney, J. R. Childress, and T. Lin, J. Appl. Phys. **89**, 6579 (2001).
[32] H. Ohldag, A. Scholl, F. Nolting, E. Arenholz, S. Maat, A. T. Young, M. Carey, and J. Stöhr, Phys. Rev. Lett. **91**, 017203 (2003).
[33] U. Nowak, K. D. Usadel, J. Keller, P. Miltényi, B. Beschoten, and G. Güntherodt, Phys. Rev. B **66**, 014430 (2002).
[34] C. Leighton, M. R. Fitzsimmons, A. Hoffmann, J. Dura, C. F. Majkrzak, M. S. Lund, and I. K. Schuller, Phys. Rev. B **65**, 064403 (2002).